PD control of magnetically actuated satellites with uneven inertia distribution

GNC 2008
7th International ESA Conference on Guidance, Navigation & Control Systems
2-5 June 2008, Tralee, County Kerry, Ireland

PD CONTROL OF MAGNETICALLY ACTUATED SATELLITES WITH UNEVEN INERTIA DISTRIBUTION

M. Wood and W. Chen
Dept. of Aeronautics and Automotive Engineering, Loughborough University, Leicestershire, LE11 3TU, UK
m.wood@lboro.ac.uk, w.chen@lboro.ac.uk

ABSTRACT

This paper considers PD attitude control of magnetically actuated satellites where one axis of inertia is considerably lower than that of the other two. The classic 'torque-projection' method of implementing the control is unsuitable for this configuration as the nature of the torque projection controller places little significance on the low inertia axis. This paper proposes a modification to the PD approach by determining the dipole moments through minimisation of a performance index rather than projection onto the magnetic field orthogonal. This allows fairer consideration of the low inertia axis and leads to improved performance of the feedback control. This approach is taken further by introducing an element of feed-forward control to improve the disturbance rejection properties of the system. In a similar way the required feed-forward compensation is determined through minimisation of an appropriate performance index. Combination of the feed-forward and feedback control successfully regulates the satellite attitude when assessed using a high fidelity simulation model. Overall this paper presents a systematic approach to the design of an effective and easy to implement attitude control system for a satellite with an uneven inertia distribution.

INTRODUCTION

The area of spacecraft magnetic attitude control is one that has attracted much recent attention in the research literature. Use of magnetic dipoles to control the attitude of a spacecraft offers a lightweight, smooth and cost-effective method of control. Although this is the case, the torque generated through use of magnetic dipoles is constrained to lie in the plane orthogonal to the local magnetic field vector, with one axis being instantaneously under-actuated. If the satellite is on an inclined orbit, suitable variation of the magnetic field allows controllability in the long term, but presents a significant challenge from a control perspective.

Within the research literature, authors investigate a number of approaches to the magnetic attitude problem. Perhaps the most popular method of control is linear quadratic regulation. By exploiting the pseudo-periodic nature of the Earth's magnetic field several authors form an optimal control problem. This type of approach is proposed in [1] when considering lateral attitude control of a momentum biased satellite. This technique is extended to full 3 axis attitude regulation in [2] and [3].

Although many of these studies present good performance, the time-varying nature of the optimal control problem requires either online solution of the time-varying Riccati equation or the storage of a large number of periodic controller gains. Although possible for satellites with more advanced onboard hardware, magnetic attitude control is frequently used for small, low-cost satellites. For these cases onboard resources are very limited and the use of complex control laws is often not possible.

For these reasons industrial applications often consider the use of simple PD schemes to regulate the satellite attitude. In [4] and [5] a PD controller is designed to calculate an ideal control torque based on the measured spacecraft pointing and angular rate. Due to the restrictions imposed by the magnetic field direction the ideal torque is projected onto the plane orthogonal to the Earth's magnetic field for implementation. In [6] and [7] the PD approach is extended to allow for time-varying controller gains while also guaranteeing asymptotic stability of the closed-loop.

The specific case of a satellite with a low inertia axis is rarely considered in the research literature. In [8] the authors note poor performance achievable using the PD approach in [1] and a modification to the commanded pitch torque is applied. This is however very much an ad-hoc approach to the problem and the issue of PD control of a satellite with an uneven inertia distribution is not fully tackled.

This paper presents a systematic approach to the design of PD controllers for satellites with an uneven inertia distribution. By considering the weaknesses of the torque projection approach, the ideal control calculated through a standard PD control is implemented through minimisation of a weighted performance index rather than direct projection onto the plane orthogonal to the Earth's magnetic field. This allows a more suitable treatment of the low inertia roll axis seen on the benchmark satellite. This PD controller is also combined with an element of feed-forward control to improve the disturbance rejection capabilities of the overall control law. Both feed-forward and feedback controller are designed and implemented using simple techniques to minimise the overall computational burden, making the strategy suitable for low-cost satellite applications.

SPACECRAFT ATTITUDE DYNAMICS

Co-ordinate System

Before introducing the spacecraft attitude dynamics an appropriate set of co-ordinate systems must be introduced. The attitude of an Earth pointing spacecraft is traditionally defined relative to a local-level reference frame. In this paper this local level reference frame is fixed at the centre of mass of the spacecraft with the *z* axis pointing towards the nadir, the *y* axis perpendicular to the orbital plane, and the *x* axis pointing approximately along the velocity vector as defined by the right hand rule. The spacecraft reference frame is also fixed at the centre of mass of the spacecraft, with the axes aligned with the principal inertia axes of the spacecraft. When the required Earth pointing attitude is achieved the spacecraft and local level reference frames are aligned.

Linearized Attitude Dynamics

The attitude dynamics of a satellite are fully described by a series of non-linear differential equations. Under certain assumptions these equations can be linearized with minimal loss of accuracy. If linearization is carried out about the Earth pointing attitude, assuming a circular orbit, small Euler angles and deviation of body rates from nominal values, the following model can be produced[9].

$$\begin{bmatrix} \dot{\phi} \\ \dot{\theta} \\ \dot{\psi} \\ \dot{\omega}_x \\ \dot{\omega}_y \\ \dot{\omega}_z \end{bmatrix} = \begin{bmatrix} 0 & 0 & 0 & 1 & 0 & 0 \\ 0 & 0 & 0 & 0 & 1 & 0 \\ 0 & 0 & 0 & 0 & 0 & 1 \\ -4\omega_0^2\sigma_1 & 0 & 0 & 0 & 0 & \omega_0(1-\sigma_1) \\ 0 & 3\omega_0^2\sigma_2 & 0 & 0 & 0 & 0 \\ 0 & 0 & \omega_0^2 & -\omega_0(1+\sigma_3) & 0 & 0 \end{bmatrix} \begin{bmatrix} \phi \\ \theta \\ \psi \\ \omega_x \\ \omega_y \\ \omega_z \end{bmatrix} + \begin{bmatrix} 0 & 0 & 0 \\ 0 & 0 & 0 \\ 0 & 0 & 0 \\ 1/J_x & 0 & 0 \\ 0 & 1/J_y & 0 \\ 0 & 0 & 1/J_z \end{bmatrix} T \quad (1)$$

ϕ, θ, ψ are the roll, pitch and yaw angles of the spacecraft reference frame with respect to the local level reference frame,
$\omega_x, \omega_y, \omega_z$ are the roll, pitch and yaw angular rates of the spacecraft reference frame about the local level reference frame,
ω_0 is the orbital frequency,
J_x, J_y, J_z are the principal inertia values about roll, pitch and yaw axes respectively,
T is the control torque applied to the satellite expressed in the spacecraft reference frame,

$$\sigma_1 = \frac{J_y - J_z}{J_x},\ \sigma_2 = \frac{J_z - J_x}{J_y},\ \sigma_3 = \frac{J_x - J_y}{J_z}.$$

Magnetic Torque Rods

The use of magnetic torque rods to regulate the attitude of a satellite introduces a time-varying component to the dynamic equations. Magnetic dipole moments interact with the Earth's magnetic field to create a control torque according to (2). Note that the cross product of these two vectors produces a torque perpendicular to the Earth's magnetic field vector, with the axis parallel to the Earth's magnetic field instantaneously under-actuated.

$$T = M \times B_{mag} \quad (2)$$

where B_{mag} is the Earth's magnetic field vector expressed in the spacecraft reference frame and M is the vector of magnetic dipole moments also expressed in the spacecraft reference frame.

The GOCE Satellite

The benchmark used throughout this investigation is the Gravity Field and Steady State Ocean Circulation Explorer (GOCE) satellite. Set for launch in 2008 GOCE is part of the ESA living planet programme. Due to its low orbit altitude of just 250km, the GOCE satellite is subject to significant external disturbances and provides an excellent benchmark for the proposed control strategy. GOCE operates at an orbital inclination of 96° and has an inertia matrix $J = diag(152 \quad 2690 \quad 2652)$. For further information regarding GOCE the interested reader may consult [8].

PD ATTITUDE CONTROL

Torque Projection PD Control

A simple yet effective technique of implementing a magnetic control law is through the so called torque projection approach. Originally proposed in [1] a PD controller is used to calculate a required control torque through equation (3).

$$T_{ideal} = -Kx \tag{3}$$

where ,
$x = [\phi \quad \theta \quad \psi \quad \omega_x \quad \omega_y \quad \omega_z]^T$,
K is a feedback gain matrix.

Due to the magnetic field constraints this torque cannot be implemented directly and is projected onto the plane orthogonal to the Earth's magnetic field vector for implementation. The resulting torque and magnetic dipole vector are defined in (4) and (5)

$$M = \frac{B_{mag} \times T}{\left|B_{mag}^2\right|} \tag{4}$$

$$T_{true} = \left(I_3 - \frac{B_{mag} B_{mag}^T}{B_{mag}^T B_{mag}} \right) T_{ideal} \tag{5}$$

where I_3 represents the 3x3 identity matrix.

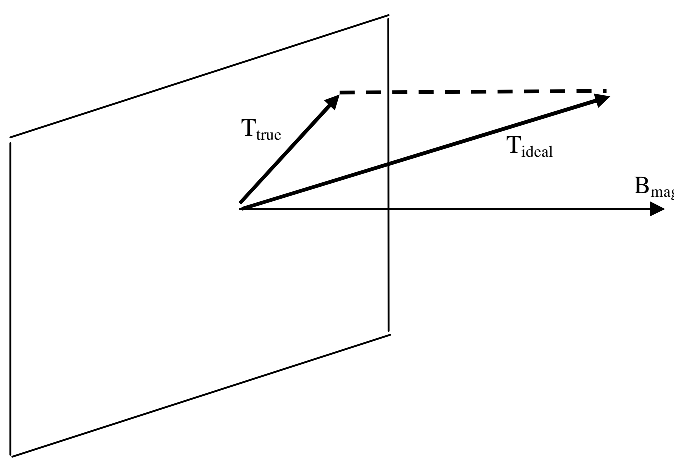

Fig. 1 – The torque projection approach

Although usually considered as a geometric approximation, the torque projection controller is in fact an implementation of a simple optimization problem. Consider minimizing the following cost function

$$\min\left(T_{ideal} - T_{true}\right)^T \left(T_{ideal} - T_{true}\right) \tag{6}$$

subject to the constraint

$$T_{true} \cdot B_{mag} = 0 \tag{7}$$

The solution of (6) subject to the constraint in (7) provides the same torque as calculated by the torque projection control and effectively minimizes the Euclidean norm of the error between the ideal and true control torques. For many configurations this is a sensible approach to the problem and yields acceptable results. When considering attitude regulation of satellites with an uneven inertia distribution the success of the torque projection controller diminishes.

Consider a simple numerical example. The GOCE satellite is controlled using a torque projection PD approach. The ideal feedback gain in (3) is chosen through pole placement technique, with the nominal closed-loop poles placed with damping ratio of 0.7 and natural frequencies $3.5\omega_0$, $0.5\omega_0$, $0.25\omega_0$. The resulting gain matrix is

$$K = \begin{bmatrix} -1.7e-4 & 0 & -2.7e-9 & 0.094 & 0 & 0.17 \\ 0 & 5.5e-2 & 0 & 0 & 15.6 & 0 \\ -4.8e-8 & 0 & -3e-3 & -0.68 & 0 & 1.6 \end{bmatrix} \tag{8}$$

Initial pointing angles of 1° are assumed about the roll and yaw axes, with angular rates of 0.001 deg/s. For the pitch axis a typical value of 0.01° pointing is assumed with 0.0001 deg/s angular rate. Applying the control law in (3)-(5), the commanded and implemented torques are summarized in Table 1. The first thing to note from Table 1 is that the commanded pitch torque is fully implemented by the torque projection controller. As the pitch axis is always controllable through one of the lateral dipole moments, control about this axis can always be implemented and demonstrates the torque projection control to be very suitable for regulation of the pitch axis.

Turning attention to the roll and yaw axes it is clear that the commanded torque about each of these axes is not successfully implemented. This is not a surprising result, as the restrictions due to the use of magnetic control will obviously limit authority of the controller. The main concern comes when analyzing the numerical values of the commanded and implemented torques and the resulting angular accelerations imparted about the roll and yaw axes.

A control torque of 36 μNm is commanded about the yaw axis which, when normalizing with respect to the yaw inertia, gives a commanded angular acceleration of 1.3×10^{-8} m/s^2. Once the torque projection has been carried out the implemented torque is reduced to just 2 μNm, with corresponding angular acceleration of 7.5×10^{-10} m/s^2. For the roll axis a torque of -1.5 μNm is commanded which, when normalizing with respect to the roll inertia, gives a commanded angular acceleration of 1.0×10^{-8} m/s^2. Note that *this acceleration is similar in magnitude to that commanded about the yaw axis even though the commanded control torque is much smaller*. Once the torque projection has been carried out the commanded torque is $+8$ μNm. This corresponds to an angular acceleration of 5.2×10^{-8} m/s^2 in the opposite direction to that commanded. Although the controller is minimizing the overall torque error, no consideration is placed on the fact that torque errors in the roll axis induce much larger acceleration errors due to the lower satellite inertia. This numerical problem leads to poor performance about the low inertia axis and needs to be addressed when considering control of satellites with uneven inertia distribution.

Table 1 – Comparison of Commanded and Implemented Torques for Torque Projection Approach

	Commanded Torque μNm	Implemented Torque μNm
Roll axis	-1.64	8.16
Pitch axis	-36.83	-36.83
Yaw axis	36.30	2.36

Weighted PD Approach

The example in the previous section shows that when minimizing the Euclidean norm of the torque error, the low inertia axis is given very low priority within this minimization process. The overall torque error may be minimized, however the effect of the error about the roll axis can be significant due to the lower inertia about this axis. In order to tackle this weakness a modification to the standard PD controller is proposed.

Derivation of Weighted PD Controller

Consider minimization of the following weighted performance index

$$\min \tfrac{1}{2}\left(T_{ideal} - T_{true}\right)^T Q\left(T_{ideal} - T_{true}\right) \tag{9}$$

subject to the constraint

$$T_{true} \cdot B_{mag} = 0 \tag{10}$$

where $Q = diag\left(\begin{bmatrix} q_1 & q_2 & q_3 \end{bmatrix}\right)$.

As the term $\tfrac{1}{2} T_{ideal}{}^T Q T_{ideal}$ is a constant, the optimization problem in (9) and (10) can be simplified to the following form.

$$-T_{ideal}^T Q T_{true} + \tfrac{1}{2} T_{true}^T Q T_{true} \tag{11}$$

subject to the constraint

$$T_{true} \cdot B_{mag} = 0 \tag{12}$$

As (11) and (12) are now in the form of a general quadratic programming problem subject to an equality constraint, it is possible to derive an explicit solution through the use of Lagrange multipliers. The necessary Lagrange conditions for this problem are

$$QT_{true} + B_{mag}\lambda - QT_{ideal} = 0 \tag{13}$$

$$B_{mag}^T T_{true} = 0 \tag{14}$$

where λ is the Lagrange multiplier (see [10]).

From (13)

$$T_{true} = -Q^{-1} B_{mag} \lambda + T_{ideal} \tag{15}$$

Substitute (15) into (14)

$$-B_{mag}^T Q^{-1} B_{mag} \lambda + B_{mag}^T T_{ideal} = 0 \tag{16}$$

Solving for the Lagrange multiplier leads to

$$\lambda = \left(B_{mag}^T Q^{-1} B_{mag}\right)^{-1} B_{mag}^T T_{ideal} \tag{17}$$

Finally, substitution of (17) into (15) yields the final solution

$$T_{true} = T_{ideal} - Q^{-1} B_{mag} \left(B_{mag}^T Q^{-1} B_{mag} \right)^{-1} B_{mag}^T T_{ideal} \tag{18}$$

For many optimization problems the matrix inverse in (18) makes the problem not numerically attractive, as the matrix $\left(B_{mag}^T Q^{-1} B_{mag}\right)$ is often ill-conditioned. For this specific optimization problem this issue is removed as the aforementioned matrix is a scalar value such that

$$\left(B_{mag}^T Q^{-1} B_{mag}\right) = \frac{B_{mag_x}^2}{q_1} + \frac{B_{mag_y}^2}{q_2} + \frac{B_{mag_z}^2}{q_3} \tag{19}$$

As the Earth's magnetic field vector will never be zero in all three directions $\left(B_{mag}^T Q^{-1} B_{mag}\right) > 0$ if $q_1, q_2, q_3 > 0$. Equation (18) can therefore be written in the more compact form

$$T_{true} = \left(I_3 - \frac{Q^{-1} B_{mag} B_{mag}^T}{\left(B_{mag}^T Q^{-1} B_{mag}\right)} \right) T_{ideal} \tag{20}$$

The equivalent dipole moment required to implement the torque is determined by (20), which can be calculated in the same way as the torque projection controller using (4). The tuning procedure itself can be simplified by considering the more specific case of a satellite with one inertia significantly lower than the other two. For the case of GOCE it is the weighting of the roll axis relative to the pitch and yaw axes that is of importance and the Q matrix is specified as

$$Q = \begin{bmatrix} q & 0 & 0 \\ 0 & 1 & 0 \\ 0 & 0 & 1 \end{bmatrix} \tag{21}$$

where $q > 0$ is the roll weighting factor.

Numerical Example

The benefits of adopting this approach can now be demonstrated by revisiting the numerical example in the previous section. The same magnetic field, state vector and ideal feedback gain are chosen, but the control signal is now implemented through (20). The roll weighting factor is chosen as $q = 8$ and the commanded and implemented torques are illustrated in Table 2.

This control approach does not miraculously allow control of both axes, but does provide a more intelligent method of implementing the control signal. Consider once again the torque about the yaw and roll axes; the implemented torque about the yaw axis is now slightly degraded from the torque projection approach, but this degradation is relatively insignificant when considering the large inertia of this axis. The control input applied about the roll axis is now much more sensible. The commanded value of -1.64 μNm cannot be achieved due to the magnetic field constraints however, due to the increased weighting within the optimization process, the controller avoids applying a large acceleration in the opposite direction to that commanded. At this particular orbit location and state vector, implementation of the desired control signal is not possible regardless of how the torque is selected. Use of the weighted PD approach avoids inducing large unwanted accelerations about the low inertia axis and is done at relatively small penalty to the yaw axis.

Table 2 – Comparison of weighted and torque projection PD control

	Commanded Torque μNm	Torque Projection μNm	Weighted PD μNm
Roll axis	-1.64	8.16	-0.33
Pitch axis	-36.83	-36.83	-36.83
Yaw axis	36.3	2.36	-0.09

The numerical example in Table 2 illustrates the motivation for the weighted PD approach. The true benefits of adopting a weighted PD controller are best demonstrated through a simulation study. The GOCE satellite is initialized at 1° pointing about each satellite axis and is considered under both torque projection PD control and the newly proposed weighted PD control. The ideal feedback gain is as defined in (8) and the roll weighting factor is chosen to be 8.

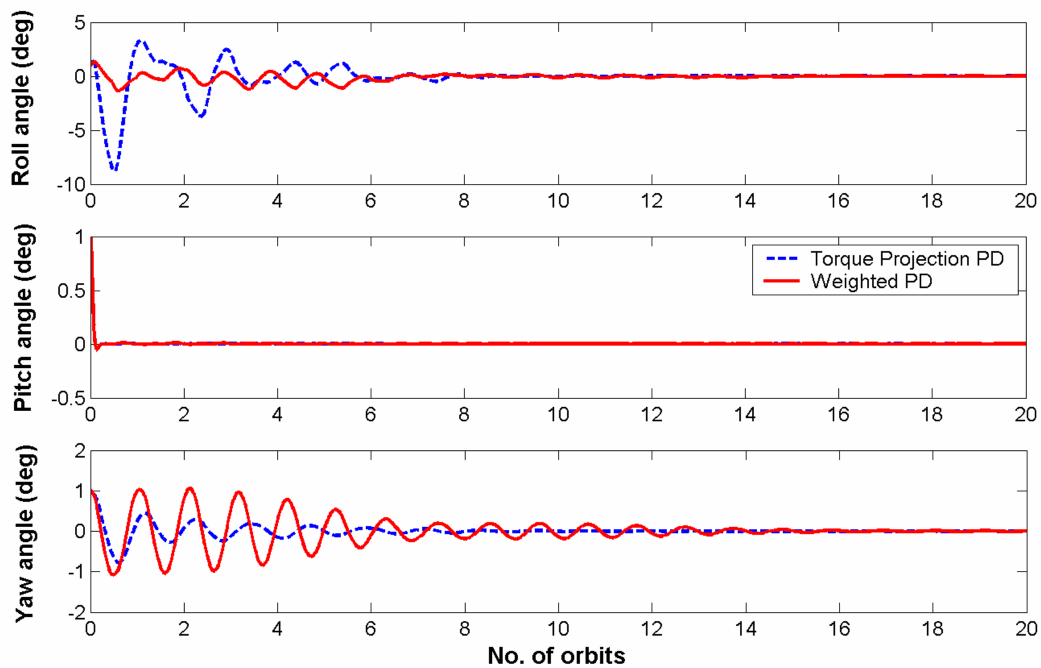

Fig. 2 – Comparison of weighted and torque projection PD controllers

The results shown in Fig. 2 support the numerical example detailed in Table 2. When both the roll and yaw errors are large, the torque projection controller places more emphasis on removal of the yaw error. This is at significant detriment to the roll axis, which at worst reaches 9° pointing error from an initial value of just 1°. As the yaw error reduces, the controller is able to restore the roll attitude, but this is clearly unacceptable performance. When the newly proposed weighted PD controller is used, the performance about the two axes is more comparable. The yaw performance is degraded (as would be expected), but this is far outweighed by the significant improvement in performance about the roll axis.

Effect of Roll Weighting Factor

The introduction of the weighted PD controller provides an additional tuning parameter to the control engineer. Selection of an appropriate weighting value is dependent on several factors.

- The ideal feedback gain: Selection of the ideal feedback gain determines the magnitude of the commanded control torques. As already discussed, it is the difference in the magnitude of the commanded torques that causes the numerical problems that bias the controller in favour of the higher inertia axes. The manner in which this feedback gain is chosen affects the control torques, and hence the weighting required to obtain acceptable performance about the low inertia axis.

- The level of performance required about the low inertia axis: If the pointing accuracy about the low inertia axis is of low importance, a low q value may be suitable to place more emphasis on performance about the other axes. If more accurate pointing is required about the low inertia axis the q value may need to be much higher for optimal performance.

- External disturbances: The level of external disturbance is very much dependent on the satellite configuration and orbit height. As well as providing suitable nominal response the feedback control must provide sufficient disturbance rejection. If too much weighting is placed on a given axis this will reduce the disturbance rejection capabilities of the other axes and can degrade performance of the overall system.

The effect of varying the weighting is demonstrated in Fig. 3. The satellite is initially at pointing angles of 1° about each axis and is controlled using a weighted PD strategy with varying *q* value.

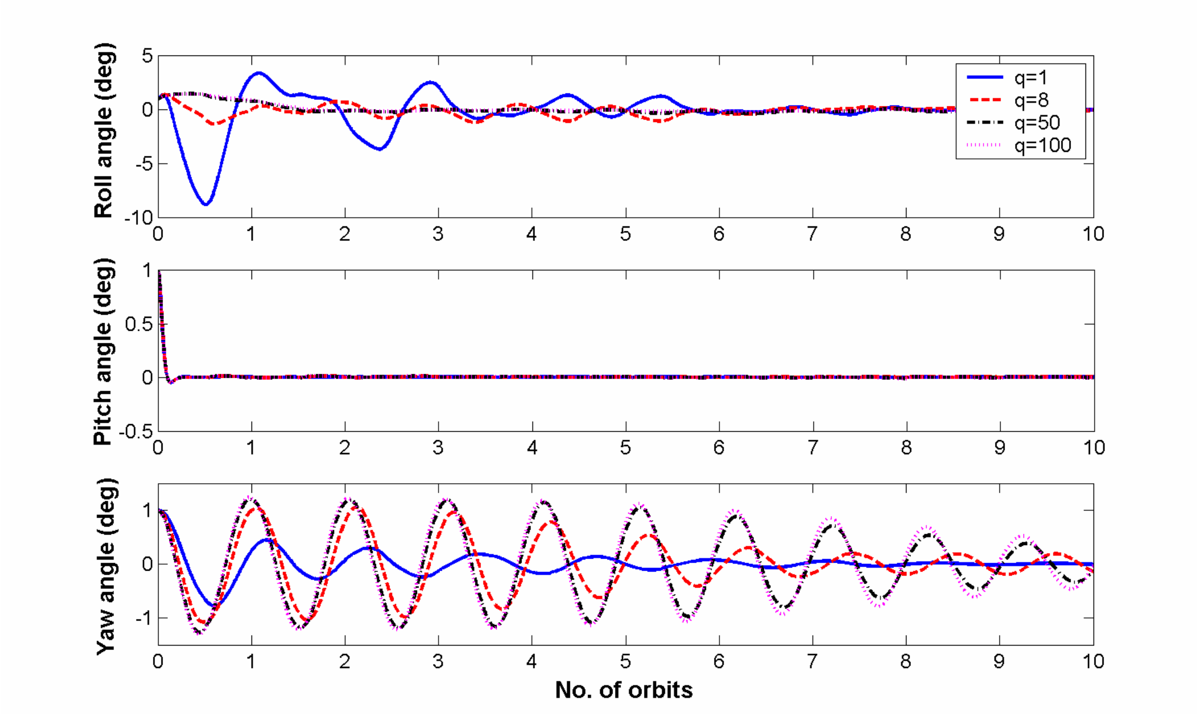

Fig. 3 – Effect of varying roll waiting factor

Selection of a low weighting factor $q = 1$ places more significance on the higher inertia axes within the optimisation. As already discussed this can lead to poor performance about the low inertia axis. Increasing the weighting factor $q = 8$ significantly improves performance about the low inertia axis at a cost of slight degradation to the yaw axis. Increasing the roll weighting further $q > 50$ places further emphasis on the low inertia axis and degrades the performance about the yaw axis.

The most important point to highlight here is that each response shown in Fig. 3 is achieved at the same ideal feedback gain. Once the ideal feedback gain has been selected, addition of the roll feedback weighting introduces a very intuitive tuning parameter that can be used to improve performance about the low inertia axis.

FEEDFORWARD DISTURBANCE COMPENSATION

For low Earth orbiting satellites, the disturbances due to the external environment can be very significant and often dominate the time response of the attitude dynamics. The feedback control proposed in the previous section can be supplemented with an element of feedforward compensation to attempt to reduce the effects of these external disturbances. Clearly the disturbances cannot be measured directly and must be estimated using a Kalman filter. As the GOCE satellite is also without rate gyros, the angular rate must also be estimated for use within the feedback controller.

Kalman Filter Design

In order to provide estimates of the external disturbances, a mathematical model of these disturbances is required. The external disturbances acting on the satellite are complex and can only be fully described by a high order Fourier decomposition. For the purpose of a state estimator this is obviously restrictive. Fortunately, analysis of the external environment shows that the primary disturbance torques occur at the frequencies $0, \omega_0$ and $2\omega_0$[1]. As a result it is these frequencies that should be considered when deriving a disturbance model. Investigations show that sufficient accuracy can even be achieved by just considering the disturbances to be constant with time.

The constant disturbance model can be defined in a discrete-time formulation as follows

$$d(k+1) = d(k) + v(k) \tag{22}$$

where $d(k)$ is the external disturbance torque and $v(k)$ is white noise.

The continuous time dynamics in (1) can be also discretized to provide the following discrete state space model.

$$x(k+1) = Ax(k) + B[u(k) + d(k)] \tag{23}$$

These two models can now be augmented to provide the following model

$$x_e(k+1) = A_e x_e(k) + B_e u(k) + \begin{bmatrix} 0_{6,3} \\ I_3 \end{bmatrix} v_1(k) \tag{24}$$

$$y_e(k) = C_e x_e(k) + D_e u(k) + w(k) \tag{25}$$

where,

$$A_e = \begin{bmatrix} A & B \\ 0_{3,3} & I_3 \end{bmatrix},\ B_e = \begin{bmatrix} B \\ 0 \end{bmatrix},\ x_e = \begin{bmatrix} x(k) \\ d(k) \end{bmatrix}$$

$$C_e = \begin{bmatrix} [I_3 \quad 0_{3,3}] & 0_{3,3} \\ [0_{3,3} \quad I_3]A & J^{-1} \end{bmatrix},\ D_e = \begin{bmatrix} 0_{3,3} \\ J^{-1} \end{bmatrix}$$

An estimate of the augmented state can then be provided through (26)

$$\hat{x}_e(k+1) = A_e \hat{x}_e(k) + B_e u(k) + L_e\left[y(k) - \left(C_e \hat{x}_e(k) + D_e u(k)\right)\right] \tag{26}$$

L_e is the Kalman filter gain matrix and is chosen to minimize the covariance of the estimation error in the usual way. $y(k)$ is the vector of measured pointing angle and acceleration and is taken directly from star sensor and accelerometer data.

Feed-Forward Compensator

Ideally the feed-forward compensator will obtain an estimate of the external disturbance using (26) and then apply an equal and opposite control torque to remove the effect of this disturbance. Unfortunately due to the reduced controllability associated with magnetic actuation this is not possible and a strategy must be derived to reduce the effects of the disturbance as much as possible. As with the feedback control, the traditional approach would be to obtain an estimate of the disturbance and then project the ideal opposing torque onto the plane orthogonal to the magnetic field vector. In a similar manner to the weighted PD controller, this approach is modified to account for the reduced inertia about the roll axis.

The ideal torque is computed from the state estimate as follows

$$T_{ideal_{FF}} = -[0_{3,6} \quad I_3]\hat{x}_e \tag{27}$$

The true feedforward torque to be implemented, T_{FF}, is then determined through minimization of the following performance index

$$\tfrac{1}{2}\left(T_{ideal_{FF}} - T_{FF}\right)^T Q_{FF}\left(T_{ideal_{FF}} - T_{FF}\right) \tag{28}$$

subject to the constraint

$$B_{mag} \cdot T_{FF} = 0 \tag{29}$$

Through an identical procedure to that carried out for the feedback control, the feedforward torque is determined through (30).

$$T_{FF} = \left(I_3 - \frac{Q_{FF}^{-1} B_{mag} B_{mag}^T}{\left(B_{mag}^T Q_{FF}^{-1} B_{mag}\right)} \right) T_{ideal_{FF}} \tag{30}$$

Unlike the feedback control, more analytical guidance can be given for the choice of Q_{FF}. The effect of the external disturbance is to impart unwanted angular accelerations about each spacecraft axis. The resulting accelerations are related to the torque and inertia through $a = J^{-1}\left(T_{ideal_{FF}} - T_{FF}\right)$. For the case of a low roll inertia, the Q_{FF} matrix can be chosen to minimize the norm of these angular accelerations through (31).

$$Q_{FF} = \begin{bmatrix} \left(J_z / J_x\right)^2 & 0 & 0 \\ 0 & 1 & 0 \\ 0 & 0 & 1 \end{bmatrix} \tag{31}$$

This approach to selection of the weighting matrix is not used for the feedback portion of the control due to the differing aims of the two control components. As the aim of the feedback control is to provide suitable closed-loop dynamics, minimisation of acceleration errors between the true and ideal case is not a meaningful design approach (minimising the acceleration error does not guarantee any particular expected closed-loop behaviour). For the feed-forward case, minimisation of accelerations is a sensible measure and hence the proposed method of selecting the Q_{FF} matrix.

Once again the motivation for this weighted minimisation can be illustrated with a very simple example. Consider the satellite at the same orbit location as described in the previous example, subject to a disturbance of 1×10^{-5} Nm about the pitch and yaw axes and 1×10^{-6} Nm about the roll axis.

Table 3 – Comparison of feed-forward strategies

	Disturbance torque after feed-forward compensation (Nm)		
Strategy	Uncompensated	Torque Projection	Weighted
Roll axis	1.0e-6	-2.6e-6	-1e-8
Pitch axis	1.0e-5	0	0
Yaw axis	1.0e-5	9.0e-6	9.7e-6

Table 3 illustrates the problems associated when the feed-forward compensation is not correctly designed. In attempting to minimise the disturbance torque about the yaw axis the torque-projection control increases the disturbance acting on the low inertia axis. This imparts large accelerations about the low inertia axis and can actually degrade the performance of the controller. The weighted feed-forward controller penalises the accelerations on each axis rather than the control torque, so ensures the low inertia axis is more appropriately dealt with. The disturbance about this axis is almost completely removed, while still removing the pitch disturbance and part of the yaw disturbance.

The numerical example in Table 3 can be reinforced with a simple simulation study. The GOCE satellite is initially at 1° pointing about each axis and is regulated using the weighted PD feedback control proposed in the previous section. The satellite is subject to a constant disturbance of 1×10^{-5} Nm about the pitch and yaw axes and 1×10^{-6} Nm about the roll axis. In order to improve the disturbance rejection properties the feedback control is augmented with a torque-projection feed-forward controller and the newly proposed weighted feed-forward controller. The combined weighted feedback and feedforward controller can be written in the closed-form shown in (32)

$$T = -\overline{K}\hat{x}_e \tag{32}$$

where

$$\bar{K}\left[\left(I_3-\frac{Q^{-1}B_{mag}B_{mag}^T}{B_{mag}^TQ^{-1}B_{mag}}\right)K\begin{bmatrix}I_6 & 0_{6,3}\end{bmatrix}+\left(I_3-\frac{Q_{FF}^{-1}B_{mag}B_{mag}^T}{B_{mag}^TQ_{FF}^{-1}B_{mag}}\right)\begin{bmatrix}0_{3,6} & I_3\end{bmatrix}\right]$$

Fig. 4 now shows the response under the control law in (32).

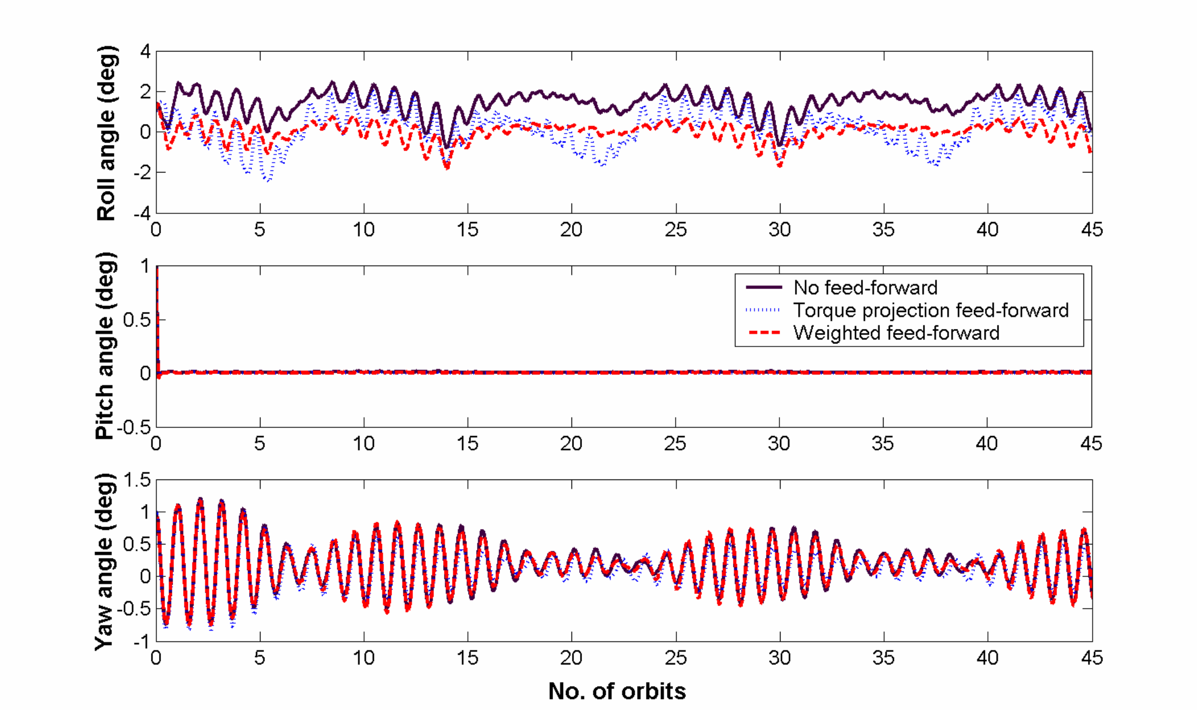

Fig. 4– Performance under varying feed-forward strategies

With feedback only control the external disturbance causes a large steady state error about the roll axis, while performance about the yaw axis is much better due to its higher inertia. The addition of the torque-projection feed-forward controller improves performance about the yaw axis however this is at the expense of the low inertia roll axis. Use of the weighted feed-forward control allows for slight improvement about the yaw axis but significantly improves the roll performance. The steady state error is removed and the nadir pointing attitude is regulated more successfully. When adopting torque projection feed-forward control, the (already well regulated) yaw axis is given high priority. The addition of the weighted feed-forward control penalises the accelerations due to the external disturbances and thus allows fairer consideration of the low inertia roll axis.

SIMULATION

Simulation Environment

To fully validate the control approach, the GOCE satellite is simulated using a high fidelity simulation model. Although the linear model in (1) has been used for controller design, a full non-linear description of the satellite dynamics is adopted for numerical simulation. The Earth's magnetic field is modelled using an 8th order IGRF model to achieve suitably high accuracy.

Due to its low Earth orbit GOCE is subject to aerodynamic drag from the upper atmosphere. This causes a perturbing torque within the attitude dynamics as the drag line is offset from the spacecraft centre of mass. This also leads to the need for an ion thruster assembly (ITA) to counteract this drag force and maintain orbital speed. This in turn further disturbs the attitude dynamics. Ideal measurements of acceleration and pointing angle are corrupted with sensor noise, while the lack of rate gyros is represented and any rate information used within the control law is obtained from the Kalman filter in (26)

Simulation Results

The GOCE satellite is simulated assuming the full disturbance and dynamics model described in the previous section. The satellite is initialised at 1° pointing about each axis at angular rate of 0.001 deg/s. To achieve best performance the roll weighting is chosen as $q = 8$ and the ideal feedback gain matrix is chosen as

$$K = \begin{bmatrix} 1e-5 & 0 & 0 & 0.2 & 0 & 0 \\ 0 & 5.5e-2 & 0 & 0 & 15.6 & 0 \\ 0 & 0 & 1e-5 & 0 & 0 & 1.6 \end{bmatrix} \tag{33}$$

Figures 5-7 show the pointing angle, magnetic dipole and Kalman filter estimate time histories.

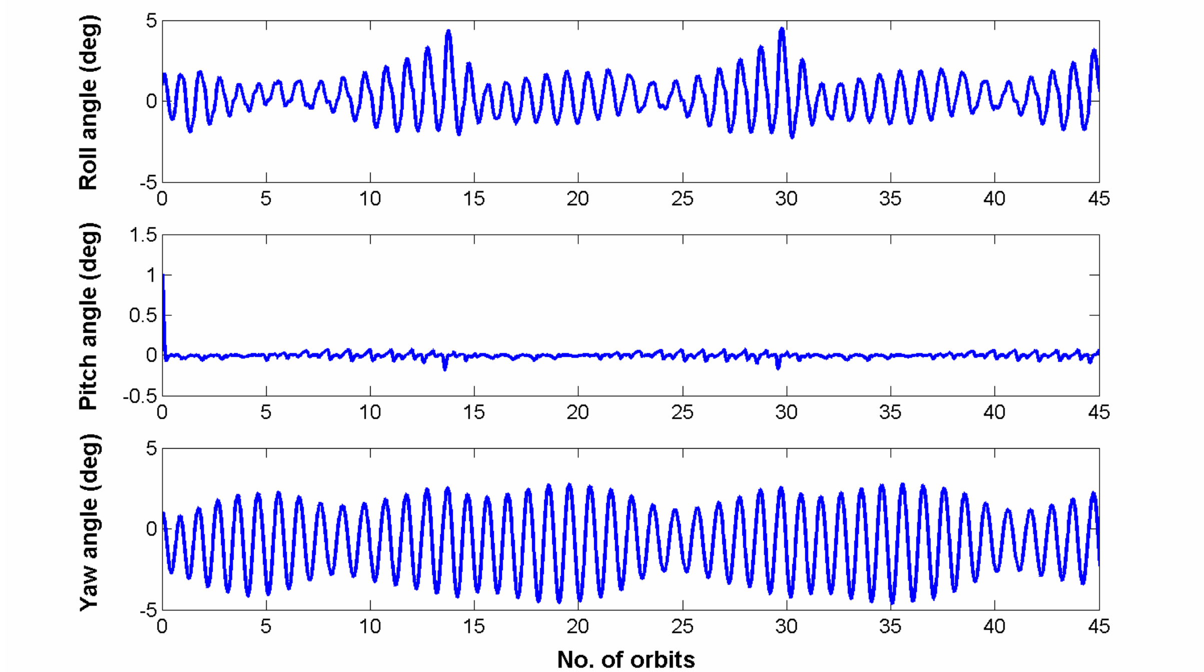

Fig. 5 – Controller performance under full disturbance model

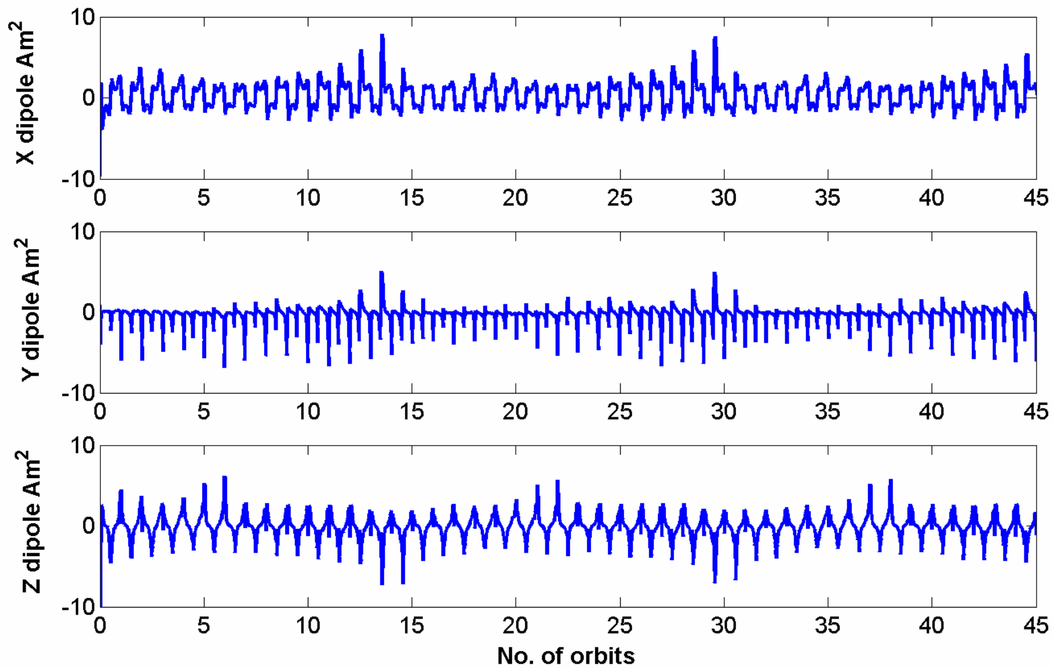

Fig. 6 – Magnetic dipole moments

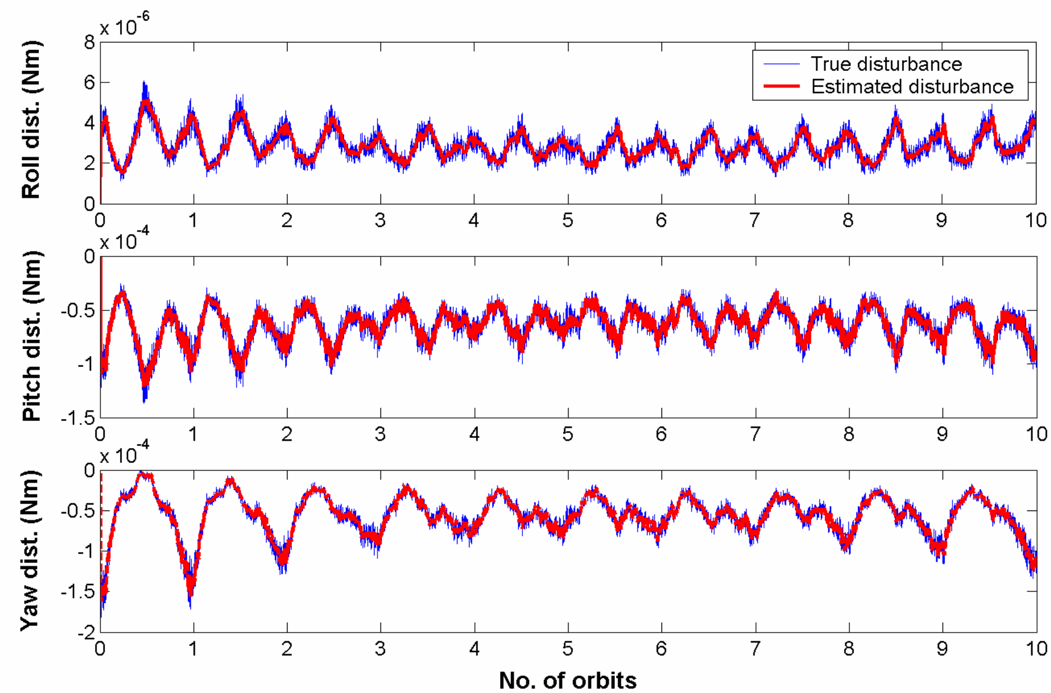

Fig. 7 – Kalman filter estimates of external disturbances

The results show the proposed strategy can effectively regulate the attitude of the GOCE satellite. Even under significant external disturbance, the attitude is regulated within 5° of the nadir. In addition Fig. 6 shows this is achieved with relatively small dipole moments. Fig. 7 also highlights the effectiveness of the simple Kalman filter design, with quite adequate results produced even with such a simple disturbance model. In the context of maintaining controller simplicity this is an interesting finding.

CONCLUSIONS

The use of PD control for the magnetic attitude control problem provides a simple and effective method of control. The classical torque projection approach is successful when applied to satellites with evenly distributed inertia, but the approach breaks down if one axis has an inertia significantly lower than that of the other two. By considering the torque-projection controller as a simple optimisation problem, an extension to this traditional control is proposed that considers minimisation of a weighted performance index to determine the true control torque to apply. This approach is taken further by adding an element of feedforward control to reduce the effect of external disturbances. The feedforward control is based on minimising the accelerations produced by the disturbance rather than the magnitude of the remaining torque. The proposed control law has been validated using a high fidelity simulation model. Even under significant external disturbance the proposed controller regulates the satellites attitude within 5° of the required value. This is done with a control approach that is very easy to implement, with even the state estimator providing suitable accuracy at minimal complexity.

REFERENCES

[1] M. Pittelkau, "Optimal periodic control for spacecraft pointing and attitude determination," *Journal of Guidance, Control, and Dynamics*, vol. 16, no. 6, pp. 1078-1084, 1993.
[2] R. Wisniewski, "Satellite Attitude Control Using Only Electromagnetic Actuation," *Ph.D Thesis*, Aalborg University, Denmark, 1996.
[3] M. Lovera, E. De Marchi and S. Bittanti, "Periodic Attitude Control Techniques for Small Satellite with Magnetic Actuators," *IEEE Transactions on Control Systems Technology*, vol. 10, no. 1, pp. 90-95, 2002.
[4] F. Martel., P. Pal,. and M. Psiaki, "Active magnetic control system for gravity gradient stabilized spacecraft," in *2nd annual AIAA/USU conference on small satellites, Logan (Utah), USA*, 1988.
[5] C. Arduini and P. Baiocco, "Active Magnetic Dampling Attitude Control for Gravity Gradient Stabilized Spacecraft," *Journal of Guidance, Control, and Dynamics*, vol. 2, no. 1, 1997.
[6] M. Lovera and A. Astolfi, "Global Magnetic Attitude Control of Spacecraft in the Presence of Gravity Gradient," *Proceedings of 42nd IEEE Conference on Decision and Control*, Maui, Hawaii, USA, 2003.
[7] M. Lovera and A. Astolfi, "Spacecraft Attitude Control Using Magnetic Actuators," *Automatica*, vol. 40, pp. 1405-1414, 2004.
[8] G. Sechi, G. Andre, D. Andreis and D. Saponara, "Magnetic Attitude Control of the GOCE Satellite," in *Proceedings of the 6th International ESA Conference on Guidance, Navigation and Control Systems*, Loutraki, Greece, 2006.
[9] M. Psiaki, "Magnetic Torquer Attitude Control via Asymptotic Periodic Linear Quadratic Regulation," *AIAA Guidance, Navigation, and Control Conference*, Denver, Colorado, USA, 2002
[10] D. Luenberger, *Linear and Non-Linear Programming*, Reading, MA, Addison-Wesley.